A 2D description of the single crystal thin plate growth from the melt by micro - pulling - down method. Part 1

Agneta M. BALINT[1], Stefan BALINT*,[2]

*Corresponding author
[1]Department of Physics, West University of Timisoara,
Blvd. V. Parvan 4, 300223 Timisoara, Romania,
balint@physics.uvt.ro
[2]Department of Computer Science, West University of Timisoara,
Blvd. V. Parvan 4, 300223 Timisoara, Romania,
stefan.balint@e-uvt.ro*

DOI: 10.13111/2066-8201.2018.10.3.4

Received: 31 May 2018/ Accepted: 25 June 2018/ Published: September 2018

Abstract: *This paper is the first part of a 2D description of a single crystal thin plate growth by micro-pulling–down (μ-PD) method. This part concerns the following aspects: the free surface equation and the pressure difference across the free surface (section 2); limits of the pressure difference p across the free surface (section 3); static stability of the free surface (section 4); the plate half thickness change rate due to the change of the pressure difference p across the free surface and the half half-thickness control (section 5).*
Numerical illustrations of the above aspects is given in case of a Si thin plate of 0.0001 [m] by using the Maple 17 software.
The advantage of this description is that it helps to better understand the dependence of the meniscus free surface shape and size on the pressure difference across the meniscus free surface and may help the automation of manufacturing.

Key Words*: modelling, thin plate growth from the melt, micro-pulling-down method*

1. INTRODUCTION

The near two-dimensional single crystal plates have attracted some attention on the applications of optical and electronic devices.

A method for growing single crystal plates from the melt is the edge-defined film-fed growth (E.F.G.) method.

The micro-pulling down (μ-PD) (Fig. 1) is a variant of the inverse EFG method and could be a second method of the single crystal thin plate growth from the melt.

In any case the micro-pulling down (μ-PD) method developed by Fukuda's laboratory in Japan [1]-[9], has been shown promising in producing single crystal fibers with good diameter control and concentration uniformity.

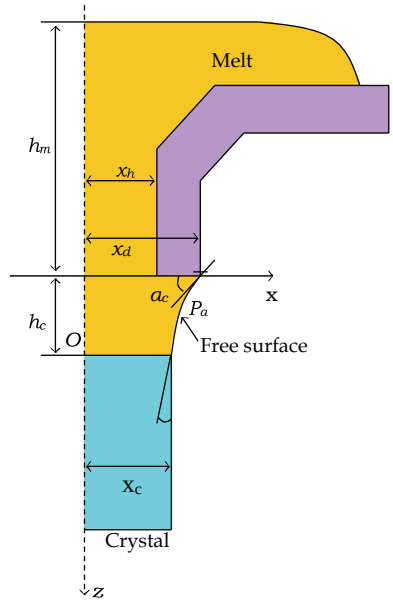

Figure 1. Schematic diagram of the μ-pulling-down plate growth process

2. THE FREE SURFACE EQUATION AND THE PRESSURE DIFFERENCE ACROSS THE FREE SURFACE IN A PD GROWTH PROCESS

The free surface of the meniscus (see Fig. 1) is described mathematically by the Young-Laplace equation [10, 11]:

$$\gamma \cdot \left(1/R_1 + 1/R_2\right) = P_a - P_b \tag{1}$$

Here: γ is the melt surface tension; $1/R_1$, $1/R_2$ denote the main normal curvatures of the free surface at a point M of the free surface; P_a is the pressure in front of the free surface; P_b is the pressure behind the free surface (Fig. 1). The pressure P_b behind the free surface is the sum of the hydrodynamic pressure p_m in the meniscus melt (due to the convection), the Marangoni pressure p_M due to the thermal Marangoni convection and the hydrostatic pressure of the melt column behind the free surface equal to $\rho \cdot g \cdot (z + h_m)$ (see Fig. 1). Here: ρ denotes the melt density; g is the gravity acceleration; z is the coordinate of M with respect to the Oz axis, directed vertically downwards; h_m denotes the melt column height between the horizontal crucible melt level and the shaper bottom level (Fig. 1). The pressure difference $P_a - P_b$ across the free surface is denoted usually by Δp and, according to the above considerations

$$\Delta p = P_a - p_m - p_M - \rho \cdot g \cdot (z + h_m) \tag{2}$$

The part p of the total pressure difference Δp given by:

$$p = -P_a + \rho \cdot g \cdot h_m + p_m + p_M \tag{3}$$

is independent of the spatial coordinate z (it can depend on the moment of time t) and the major part of p is $-P_a + \rho \cdot g \cdot h_m$. That is because the sum $p_m + p_M$ in general is small with

respect to $-P_a+\rho\cdot g\cdot h_m$. For this reason thereafter it is assumed that the pressure difference p is given by:

$$p=-P_a+\rho\cdot g\cdot h_m \tag{4}$$

Remark that the pressure difference p given by (4) can be controlled by P_a and h_m. With this approximation the Young-Laplace free surface equation (1) can be written as:

$$\gamma\cdot\left(1/R_1+1/R_2\right)=-\rho\cdot g\cdot z-p \tag{5}$$

Therefore, for a meniscus free surface which is symmetric with respect to the vertical plane YOZ and is independent on the coordinate *y* [10], [11], the differential equation of the meridian curve of the free surface is given by:

$$z''=-\frac{\rho\cdot g\cdot z+p}{\gamma}\left[1+\left(z'\right)^2\right]^{3/2};\quad x_c\le x\le x_d \tag{6}$$

where x_c is the tape half-thickness and x_d is the shaper half-thickness, respectively.

The function $z(x)$, describing the meridian curve profile, verifies the following boundary conditions:

$$z'(x_c)=-\tan\left(\pi/2-\alpha_g\right);\qquad z(x_c)=h_c>0 \tag{7}$$

$$z'(x_d)=-\tan\alpha_c;\qquad z(x_d)=0 \tag{8}$$

$$z(x)\text{ is strictly decreasing on }[x_c,x_d] \tag{9}$$

The first condition in (7) expresses that at the three phase point (x_c,h_c), where the thermal conditions for solidification have to be realized (h_c is the crystallization front level), the angle between the tangent line to the meridian curve of the free surface and the vertical is equal to the growth angle α_g. If this condition is satisfied during the whole growth process, then the plate thickness is constant. The second condition in (7) expresses that the height of the crystallization front is equal to $h_c>0$. The first condition in (8) expresses that at the point $(x_d,0)$, where the meridian curve touches the outer edge of the shaper, the catching angle (contact angle) is equal to α_c. The second condition in (8) expresses that at the point $(x_d,0)$ the meridian curve is fixed to the outer edge of the shaper. Condition (9) expresses that the meniscus shape is relatively simple. For the static stability of the free surface the function $z(x)$, describing the meridian curve profile, beside the conditions (6), (7), (8) and (9), has to minimize the functional of the free energy of the melt column behind the free surface [10], [11], given by:

$$I(z)=\int_{x_c}^{x_d}\left\{\gamma\cdot\left[1+\left(z'\right)^2\right]^{1/2}-\frac{1}{2}\cdot\rho\cdot g\cdot z^2-p\cdot z\right\}dx \tag{10}$$

Note that only statically stable free surface can exist in the real world. Equations (6)-(10) define a part of the 2D model of the process.

3. LIMITS OF THE PRESSURE DIFFERENCE p IN A μ-PD GROWTH PROCESS

If p is arbitrary, then it can happen that there is no function $z(x)$ defined for $x \in [x_c, x_d]$ which verifies (6) - (9) and supplementary $z''(x) > 0$. This means that there is no convex static meniscus symmetric with respect to the plane YOZ having convex meridian curve independent on *y*. The following statement is a necessary condition for the existence of a function $z(x)$ having the properties (6) - (9) and $z''(x) > 0$ for $r \in [x_c, x_d]$.

Statement 1. *If* $\alpha_c + \alpha_g < \pi/2$ *and there are* $z(x)$ *defined for* $x \in [x_c, x_d]$ *which verifies (6) - (9) and* $z''(x) > 0$, *then* p *satisfies:*

$$\gamma \cdot \frac{\alpha_c + \alpha_g - \pi/2}{x_d} \cdot \frac{n}{n-1} \cdot \cos\alpha_c - \rho \cdot g \cdot x_d \cdot \frac{(n-1)}{n} \cdot \tan(\pi/2 - \alpha_g) \le p \le \gamma \cdot \frac{\alpha_c + \alpha_g - \pi/2}{x_d} \cdot \frac{n}{n-1} \cdot \sin\alpha_g \tag{11}$$

where $n = x_d / x_c > 1$.

The proof of this statement can be found in **Appendix**. In the following we show how to use the above inequalities to create a convex static meniscus that is symmetric to the plane YOZ having convex meridian curve independent on *y*.

For instance, in case of a thin Si plate the following numerical data are used [12], [13]: $x_d = 2\times10^{-4}[m]$; $\alpha_c{}^1 = 0.523[rad]$; $\alpha_g = 0.192[rad]$; $\rho = 2.58\times10^3[kg/m^3]$; $g = 9.81[m/s^2]$; $\gamma = 0.765$ [N/m] and $x_c = 1\times10^{-4}[m]$.

The pressure limits appearing in (11) (Statement 1) are denoted by:

$$L_1(n) = \gamma \cdot \frac{\alpha_c + \alpha_g - \pi/2}{x_d} \cdot \frac{n}{n-1} \cdot \cos\alpha_c - \rho \cdot g \cdot x_d \cdot \frac{(n-1)}{n} \cdot \tan(\pi/2 - \alpha_g) \tag{12}$$

$$L_2(n) = \gamma \cdot \frac{\alpha_c + \alpha_g - \pi/2}{x_d} \cdot \frac{n}{n-1} \cdot \sin\alpha_g \tag{13}$$

For n in the range $[1.01, 10]$ these limits are represented in Fig. 2.

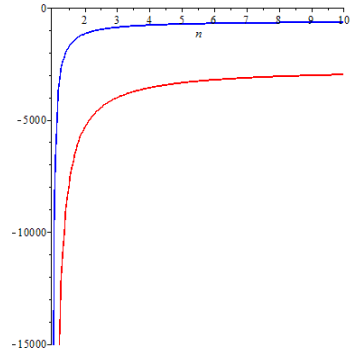

Figure 2. The pressure limits for $n \in [1.01, 10]$: the lower limit $L_1(n)$ (red curve), the upper limit $L_2(n)$ (blue curve)

For $x_c = x_d/2$ the value of n is $n = x_d/x_c = 2$ and the pressure limits are $L_1(2)$ = - 5350.677670 [*Pa*]; $L_2(2)$ = - 1175.797552 [*Pa*]. So, the values of *p* have to be in the range of [- 5350.677670; - 1175.797552] [*Pa*]. In practice, the value of $p = -P_a + \rho \cdot g \cdot h_m$ can be controlled through the values of P_a and h_m. But the values of p should range in a large interval and we don't know which value of p is appropriate. Moreover, it is not sure that in the above range there is a value of p for which a meniscus exists which is symmetric to the YOZ plane independent on *y* and with convex meridian curve (the condition (11) is only necessary). In order to answer these questions the following initial value problem:

$$\begin{cases} \dfrac{dz}{dx} = -\tan\alpha \\ \dfrac{d\alpha}{dx} = \dfrac{\rho \cdot g \cdot z + p}{\gamma} \cdot \dfrac{1}{\cos\alpha} \\ z(x_d) = 0, \quad \alpha(x_d) = \alpha_c \end{cases} \tag{14}$$

has to be solved numerically for different values of the pressure difference p in the range [- 5350.677670; - 1175.797552] [*Pa*]. In this way a family of solution is obtained $z = z(x, p)$, $\alpha = \alpha(x, p)$ depending on p. That value of p is good for which the growth angle is achieved at x_c; i.e. $z'(x_c, p) = -\tan(\pi/2 - \alpha_g)$. In this way it is found that the value of p is p = - 3472.5 [*Pa*] for this value of p at $x_c = 1\times10^{-4}[m]$ the growth angle α_g is achieved; i.e. $\alpha(x_c) = \pi/2 - \alpha_g = 1.37871023884957$ [*rad*]. For this value of p the level of the crystallization front $z(x_c) = h_c$ is $h_c = 1.4011\times10^{-4}[m]$. The profile of the meridian curve of the meniscus $z = z(x)$ in this case is presented in Fig. 3a and the variation of $\alpha(x)$ in Fig. 3b.

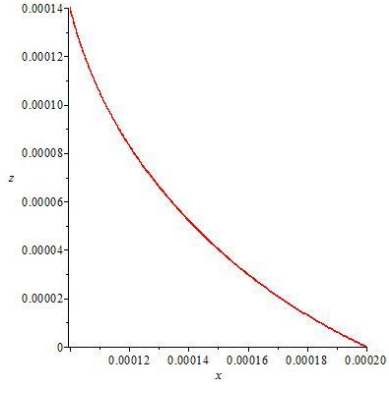

Figure 3a. Meridian curve shape $z = z(x)$
p = -3472.5[*Pa*], $x_c = 1\times10^{-4}[m]$
$h_c = 1.4011\times10^{-4}[m]$.

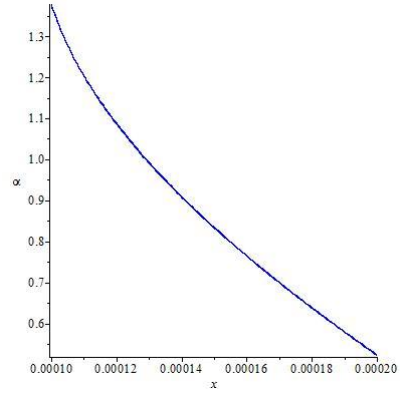

Figure 3b. Variation of $\alpha(x)$
$\alpha(x_c, p) = 1.37871023884957$ [*rad*]

Computation reveals that in the considered range there is no other value of p such that for $x_c = 1\times10^{-4}[m]$, $\alpha(x_c) = \pi/2 - \alpha_g = 1.37871023884957$ [*rad*]. At this point it has to be

noted that the downward orientation of the OZ axis in Fig. 1. and the upward orientation of the OZ axis in figures Fig. 3a; Fig. 4a; Fig. 5a; Fig. 6a; Fig. 7a; Fig. 9a; Fig. 10a; Fig. 12a; Fig. 13a are opposite. For that, these last figures have to be rotated with 180 degrees around the OX axis in order to obtain the meridian curve shape as presented in Fig. 1.

Remark. The same computation reveals that for different values of p in the range [- 5350, - 1737.9] [Pa] there are different values of $x_c(p)$ for which $\alpha(x_c)=\pi/2-\alpha_g=$ 1.37871023884957 [rad]. More than that, when p increases from value of - 5350 [Pa] to value of - 1737.9 [Pa] then $x_c(p)$, having the above property, decreases from value of 0.0001351 [m] to value of 0.00000001 [m] and $z(x_c(p))=h_c(p)$ increases from value of 0.00009094869 [m] to value of 0.00028024634269 [m]. For p = -5350 [Pa] the meridian curve of the corresponding meniscus $z=z(x,p)$ is presented in Fig. 4a and the variation of $\alpha(x,p)$ in Fig. 4b.

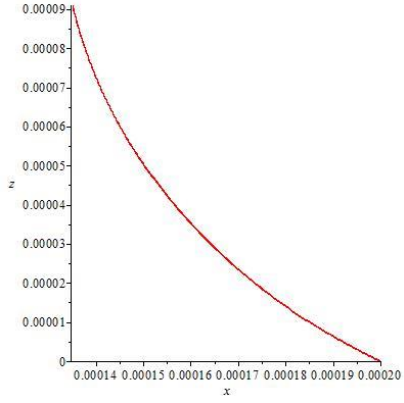

Figure 4a. Meridian curve shape $z=z(x,p)$
p = - 5350 [Pa], $x_c(p)=0.00001351$ [m]
$h_c(p)=0.00009094869$ [m]

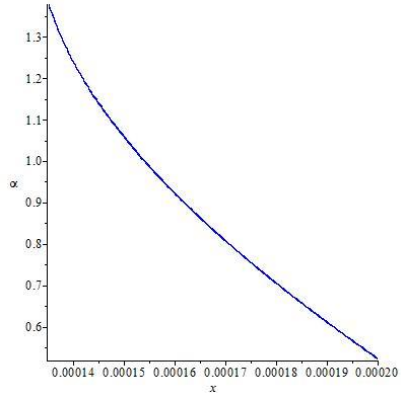

Figure 4b. Variation of $\alpha(x,p)$
$\alpha(x_c)=1.37871023884957$ [rad]

For p = - 1737.9 [Pa] the meridian curve of the corresponding meniscus $z=z(x,p)$ is presented in Fig. 5a and the variation of $\alpha(x,p)$ in Fig. 5b.

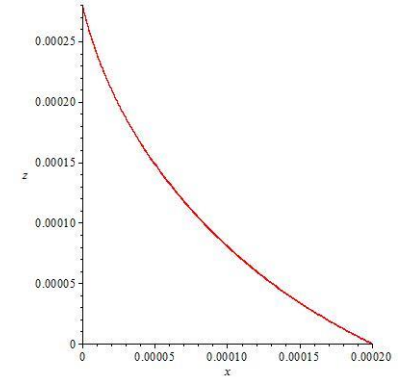

Figure 5a. Meridian curve shape $z=z(x,p)$
p = - 1737.9 [Pa], $x_c(p)=0.00000001$ [m]
$h_c(p)=0.00028024634269$ [m]

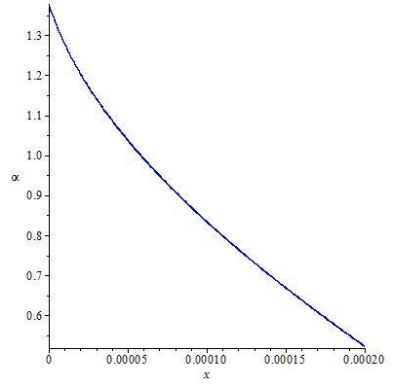

Figure 5b. Variation of $\alpha(x,p)$
$\alpha(x_c)=1.37871023884957$ [rad]

In other words, the computation reveals that to any p in the range [- 5350, - 1737.9] [*Pa*] corresponds a meniscus which is symmetric to the YOZ plane independent on y and with convex meridian curve $z = z(x, p)$, but for only one of them, namely for p = - 3472.5 [*Pa*], the following equality holds $x_c = 0.0001[m]$. The computation reveals also that to any p in the range [- 5350, - 3472.5] [*Pa*] corresponds a static meniscus such that the corresponding plate half thickness $x_c(p)$ satisfies $x_c(p) > 0.0001[m]$ and to any p in the range [- 3472.5, - 1737.9] [*Pa*] corresponds a static meniscus such that the corresponding plate half thickness satisfies $x_c(p) < 0.0001[m]$. So, for any p in the range [- 3472.5, - 1737.9] [*Pa*] it makes sense to compute $\alpha(0.0001, p)$ and $z(0.0001, p)$. Moreover, although $x_c(p) > 0.0001[m]$, for any p in the range [-3601,- 3472.5)[*Pa*] it makes sense, to compute $\alpha(0.0001, p)$ and $z(0.0001, p)$. For p = - 3601 [*Pa*] the results of this computation are represented in Fig. 6a and Fig. 6b, respectively. For p = - 1737.9 [*Pa*] the results of this computation are represented in Figs. 7a and 7b.

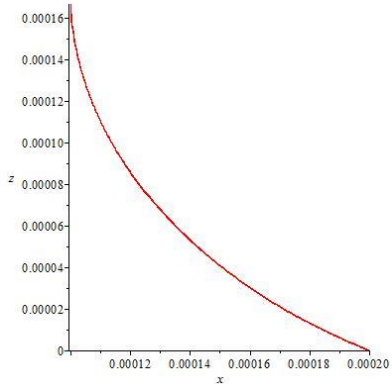

Figure 6a. Meridian curve shape $z = z(x, p)$
p = - 3601 [*Pa*],
$z(0.0001, p) = 0.00016667473381311$ [*m*]

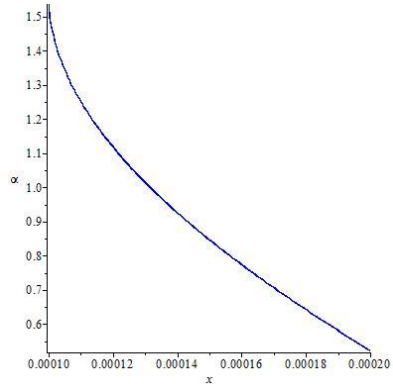

Figure 6b. Variation of $\alpha(x, p)$
p = - 3601 [*Pa*]
$\alpha(0.0001, p) =$ 1.53759729718637 [*rad*]

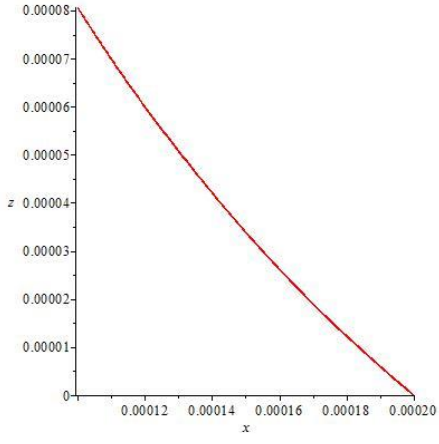

Figure 7a. Meridian curve shape $z = z(x, p)$
p = - 1737.9 [*Pa*]
$z(0.0001, p) =$ 0.0000806366424196828 [*m*]

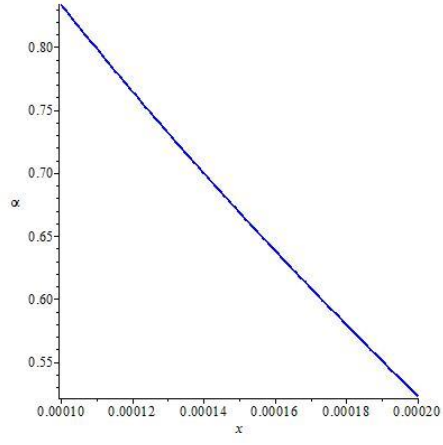

Figure 7b. Variation of $\alpha(x, p)$
p = - 1737.9 [*Pa*]
$\alpha(0.0001, p) = 0.834161904617903$ [*rad*]

The angle $\alpha(0.0001, p)$, considered above, is the angle made by the line tangent to the meniscus corresponding to p, at the point $(0.0001, z(0.0001, p)$, with the horizontal axis. This angle is equal to $\pi/2-\alpha_g = 1.37871023884957$ [*rad*] if and only if p = - 3472.5 [*Pa*].

For any p in the range [- 3601, - 3472.5] [*Pa*] the angle $\alpha(0.0001, p)$ satisfies $\alpha(0.0001, p) > \pi/2-\alpha_g = 1.37871023884957$ [*rad*]. For p in the range [- 3472.5, - 1737.9] [*Pa*] the angle $\alpha(0.0001, p)$ satisfies $\alpha(0.0001, p) < \pi/2-\alpha_g = 1.37871023884957$ [*rad*]. If p is different from p = - 3472.5 [*Pa*], then the difference $\alpha(0.0001, p)-(\pi/2-\alpha_g) = \alpha(0.0001, p)$ - 1.37871023884957 [*rad*] represents the deviation from the growth angle, due to the deviation of the pressure difference p from the value p = - 3472.5 [*Pa*]. For p in the range [-3601,- 3472.5) [*Pa*] the deviation is strictly positive and for p in the range (-3472.5,- 1737.9)[*Pa*] the deviation is strictly negative.

4. STATIC STABILITY OF THE FREE SURFACE IN A PD GROWTH PROCESS

This section deals with the static stability of the free surface [11].The following statement is a sufficient condition of static stability of the free surface.

Statement 2. *Under the conditions appearing in Statement1, if* $n = x_d / x_c > 1$ *satisfies*

$$\frac{1}{n} < \pi \cdot \frac{1}{x_d} \cdot \frac{\gamma^{1/2} \cdot \sin^{3/2} \alpha_g}{\rho^{1/2} \cdot g^{1/2}} \tag{15}$$

then the convex meniscus symmetric to the YOZ plane and independent on y is stable, i.e. $z(x)$ *minimizes the free energy functional* $I(z)$.

The proof of this statement can be found in **Appendix**. In the case of the thin *Si* plate considered in Section 3 we have: $1/n = 0.5$ and $\pi \cdot \frac{1}{R_d} \cdot \frac{\gamma^{1/2} \cdot \sin^{3/2} \alpha_g}{\rho^{1/2} \cdot g^{1/2}} = 7.198643944$.

Therefore, the static free surface is stable.

5. EQUATION OF THE PLATE HALF THICKNEES CHANGE RATE DUE TO THE CHANGE OF THE PRESSURE DIFFERENCE IN A PD GROWTH PROCESS

Starting from the condition of growth angle constancy according to [11] the following equation of the plate half thickness change rate, due to the pressure difference perturbation p is obtained:

$$\begin{aligned} &dx_c / dt = -v \tan(\alpha(0.0001, p)-(\pi/2-\alpha_g)) \\ &x_c(0) = 0.0001 \end{aligned} \tag{16}$$

Here $x_c(t)$ is the tape half thickness at the moment of time t, v for the moment is a strictly positive constant (the pulling rate) and $\alpha(0.0001, p)$ is the angle between the line

tangent to the meridian curve of the perturbed meniscus at the point of coordinates $(0.0001, z(0.0001, p))$, and the horizontal axis. If p = - 3472.5 [Pa], then $\alpha(0.0001, p) = \pi/2 - \alpha_g$. So, $\tan(\alpha(0.0001, p) - (\pi/2 - \alpha_g)) = \tan(0) = 0$ and the initial value problem (16) becomes:

$$\begin{aligned} dx_c / dt &= 0 \\ x_c(0) &= 0.0001 \end{aligned} \tag{17}$$

For p = - 1737.9 [Pa] we have $\alpha(0.0001, p)$ ==0.834161904617903.
So, $-v \tan(\alpha(0.0001, p) - (\pi/2 - \alpha_g))$ =- $v \tan($ - 0.5446344224) and (5.1) becomes:

$$\begin{aligned} dx_c / dt &= v \tan(0.5446344224) \\ x_c(0) &= 0.0001 \end{aligned} \tag{18}$$

For p = - 3601 [Pa] we have $\alpha(0.0001, p)$ =1.53759729718637.
So, $-v \cdot \tan(\alpha(0.0001, p) - (\pi/2 - \alpha_g)) = -v \cdot \tan$ (0.15880097) and (16) becomes:

$$\begin{aligned} dx_c / dt &= -v \tan(0.15880097) \\ x_c(0) &= 0.0001 \end{aligned} \tag{19}$$

For $v = 0.0001[m/s]$] the solutions of the initial value problems (17), (18) and (19) are represented on Fig. 8 with green, blue and red, respectively.

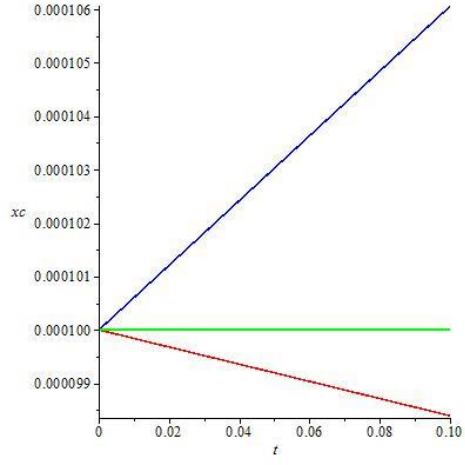

Figure 8. The plate half thickness change for $v = 0.0001[m/s]$, p = - 3472.5 [Pa] (green), p = - 3601 [Pa] (red), and p = - 1737.9 [Pa] (blue), respectively

On Fig. 8. can be seen that:
- if p is constantly equal to - 3472.5 [Pa] in the first $0.1[s]$, then the plate half thickness is equal to $x_c = 0.0001[m]$ (colour green).
- if at $t = 0$, p decreases instantaneously from - 3472.5 [Pa] to - 3601 [Pa], then the plate half thickness decreases in $0.1[s]$ from $x_c = 0.0001[m]$ to x_c'= 0.000098398505586 [m] (colour red).

- if at $t = 0$, p increases instantaneously from - 3472.5 [Pa] to – 1737.9 [Pa], then the plate half thickness increases in 0.1[s] from $x_c = 0.0001[m]$ to x_c''= 0.000106057468617 [m] (colour blue).

In the two cases when the half thickness $x_c = 0.0001[m]$ varies due to the pressure perturbation a problem appears: "what is the procedure which has to be applied in order to recover the half thickness $x_c = 0.0001[m]$"?

In the following two procedures are presented:

a). the recovery of the value $x_c = 0.0001[m]$ starting from the value x_c''= 0.000106057468617 [m].

b). the recovery of the value $x_c = 0.0001[m]$ starting from the value x_c'= 0.000098398505586 [m].

Both procedures are based on the pressure difference value modification at the moment of time $t = 0.1[s]$.

a). The first step in this procedure is the determination of the static meniscus for which the half thickness is x_c''= 0.000106057468617 [m]. This means in fact the determination of the pressure difference p'' for which the half thickness is x_c''. Computation shows that $p'' = -3696.39[Pa]$ and the results are presented in Figs. 9a and 9b.

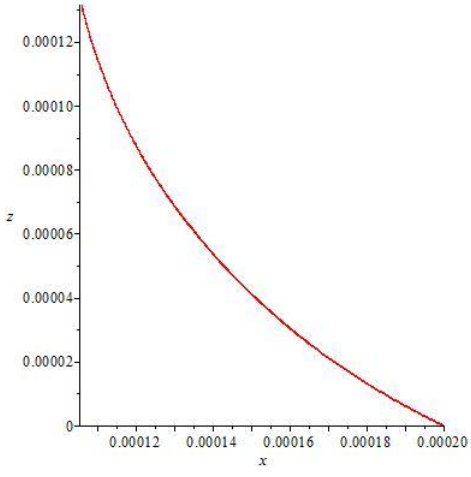

Figure 9a. **M**eridian curve shape $z = z(x, p'')$
$p'' = -3696.39[Pa]$
$z(x_c'', p'') = h_c'' =$ 0.000131635404585648 [m]
x_c''= 0.000106057468617 [m]

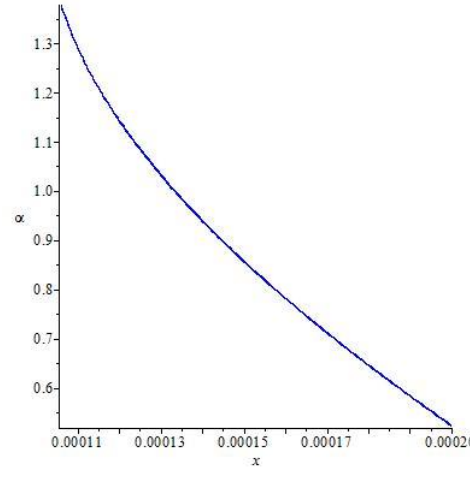

Figure 9b. Variation of $\alpha(x, p'')$
$p'' = -3696.39[Pa]$
$\alpha(x_c'', p'') =$ 1.37879883721489 [rad]

The second step in this procedure is to find a perturbation p of p'' for which the half thickness x_c''= 0.000106057468617 [m] decreases. We have to look for a value of p less than p''.

For example for $p = -3800[Pa]$, computation reveals that $z = z(x, p)$ and $\alpha(x, p)$ vary as in Figs. 10a and 10b, which show that x_c'' will decrease.

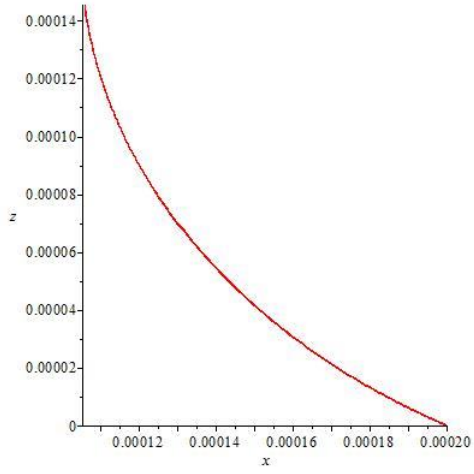

Figure 10a. Meridian curve shape $z = z(x, p)$
$p = -3800[Pa]$
$z(x_c'', p) =$ 0.000145555762785026 [m]
$x_c'' =$ 0.000106057468617 [m]

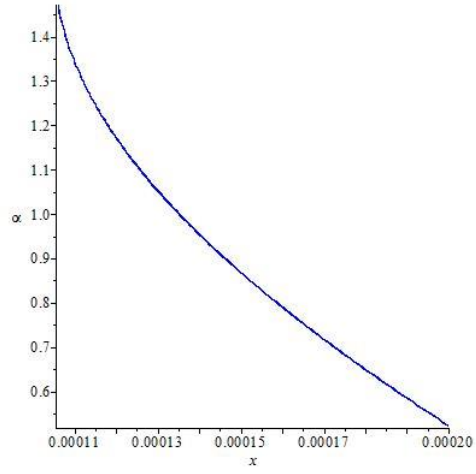

Figure 10b. Variation of $\alpha(x, p)$
$p = -3800[Pa]$
$\alpha(x_c'', p) =$ 1.4721619552749 [rad]

For the value $p = -3800[Pa]$ starting from $x_c'' =$ 0.000106057468617 [m] at the moment of time $t = 0.1[s]$ the decrease of x_c'' is described by the solution of the initial value problem

$$dx''_c / dt = -v\tan(0.093365628)$$
$$x_c''(0.1) = 0.000106057468617 \quad (20)$$

The decrease of x_c'' and the complete recovery of $x_c = 0.0001[m]$ are presented in Figs. 11.

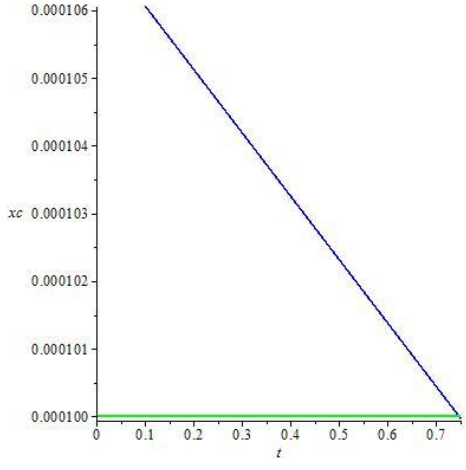

Figure 11a. Decrease of $x_c''(t)$ for t in the range $[0.1, 0.75][s]$

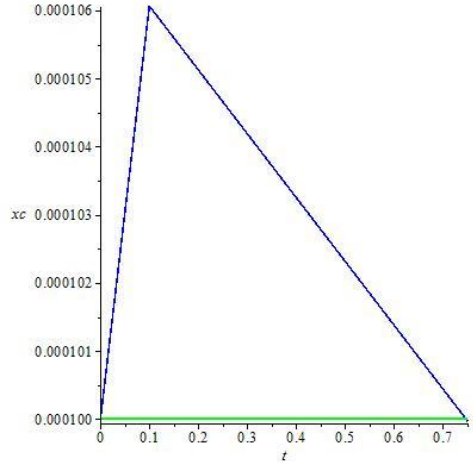

Figure 11b. Increase from $x_c = 0.0001[m]$ to $x_c'' =$ 0.000106057468617 [m] and the recovery of $x_c = 0.0001[m]$.

b). The first step in this procedure is to establish the static meniscus for which the half thickness is $x_c' =$ 0.000098398505586 [m].This means in fact to establish the pressure

difference p' for which the stable meniscus half thickness is x_c'. Computation shows that we have to take $p' = -3417.9[Pa]$ and the result is presented in Figs. 12.

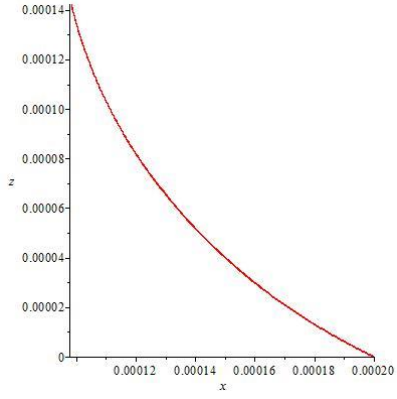

Figure 12a. Meridian curve shape $z = z(x, p')$
$p' = -3417.9[Pa]$
$x_c' = 0.000098398505586\ [m]$
$z(x_c', p') = h_c' = 0.000142368182337325\ [m]$

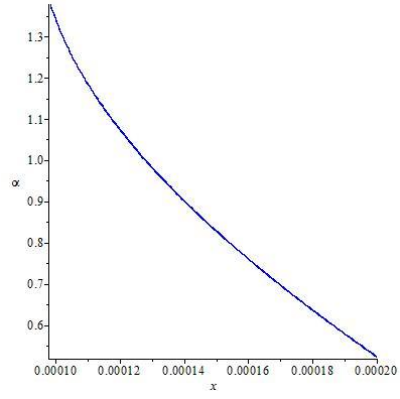

Figure 12b. Variation of $\alpha(x, p')$
$p' = -3417.9[Pa]$
$\alpha(x_c', p') = 1.37879883721489\ [rad]$

The second step in this procedure is to find a perturbation p of p' for which the half thickness $x_c' = 0.000098398505586\ [m]$ increases. For that we have to look for p whose value is greater than p'. For example, if we take $p = -3300[Pa]$, computation reveals that $z = z(x, p)$ and $\alpha(x, p)$ vary according to Figs. 13a and 13b, showing that x_c' will increase.

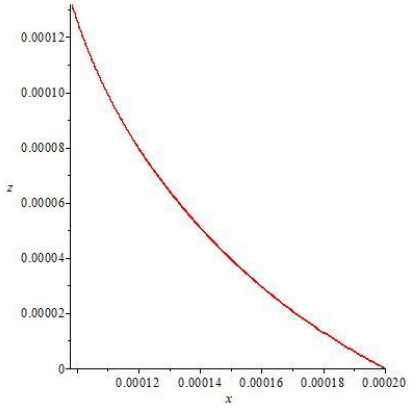

Figure 13a. Meridian curve shape $z = z(x, p)$,
$p = -3300[Pa]$
$z(x_c', p) = 0.000131854329762203\ [m]$
$x_c' = 0.000098398505586\ [m]$

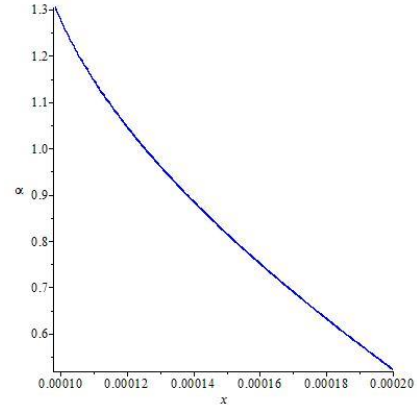

Figure 13b. Variation of $\alpha(x, p)$
$p = -3300[Pa]$
$\alpha(x_c', p) = 1.30540344368778\ [rad]$

For $p = -3300[Pa]$ starting from $x_c' = 0.000098398505586\ [m]$ at the moment of time $t = 0.1[s]$ the increase of x_c' is described by the solution of the initial value problem:

$$\begin{aligned} dx_c'/dt &= -0.0001 \cdot \tan(-0.073392883) \\ x_c'(0.1) &= 0.000098398505586 \end{aligned} \tag{21}$$

The increase of x_c' and the complete recovery of $x_c = 0.0001[m]$ are presented in Figs. 14.

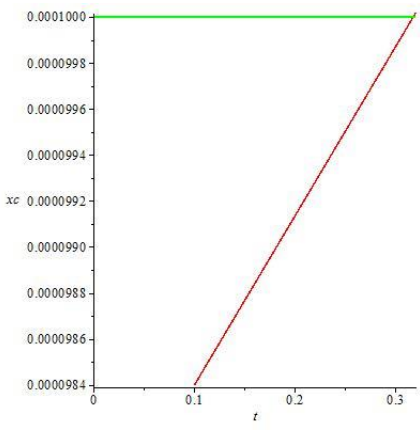

Figure 14a. Increase of $x_c'(t)$ For t in the range [0.1, 0.33] [s]

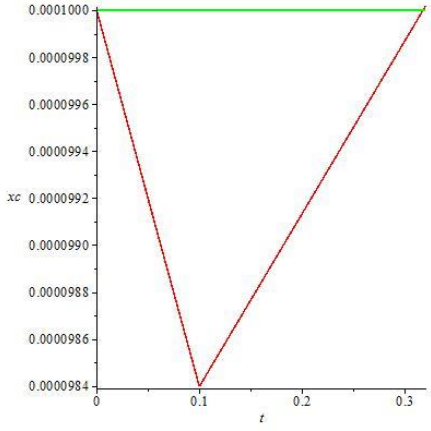

Figure 14b. Decrease from $x_c = 0.0001[m]$ to $x_c' = 0.000098398505586$ [m] and the recovery of x_c

If $p = p(t)$ oscillates around the value $-3472.5[Pa]$, then $\alpha(0.0001, p)$ oscillates around the value $\pi/2 - \alpha_g$. In this case the plate half thickness evolution is described by the solution of the initial value problem:

$$\begin{aligned} &dx_c/dt = -v\tan(\alpha(0.0001, p(t)) - (\pi/2 - \alpha_g)) \\ &x_c(1) = 0.0001 \end{aligned} \tag{22}$$

For $v = 0.0001[m/s]$ and $\alpha(0.0001, p(t)) = \pi/2 - \alpha_g + 0.001\sin(6t)$ the plate half thickness evolution during the first second can be seen in Fig. 15a. In Fig. 15b the plate half thickness evolution during the first second is presented for the already considered instantaneous perturbations and for the above considered time dependent perturbation.

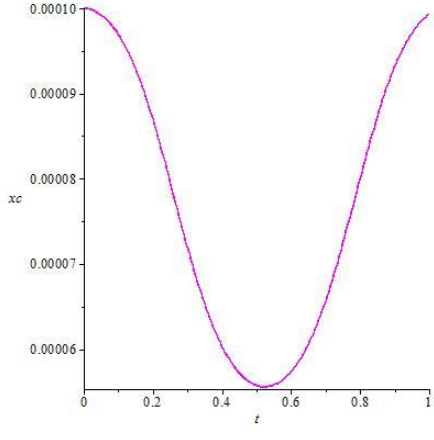

Figure15a. The plate half thickness change for $\alpha(0.0001, p(t)) = \pi/2 - \alpha_g + 0.001\sin(6t)$

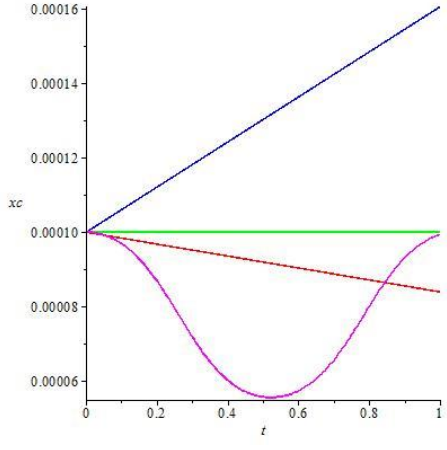

Figure15b. The plate half thickness change for $v = 0.0001[m/s]$,
p = - 3472.5 [Pa] (green)
p = - 1737.9 [Pa] (red), p = - 3601 [Pa] (blue)
$\alpha(0.0001, p(t)) = \pi/2 - \alpha_g + 0.001\sin(6t)$ (magenta)

6. CONCLUSIONS

In the framework of the presented description, the following quantities, related to the micro tape growth process from the melt by pulling down method, can be computed:

- pressure difference across the free surface to create a stable static meniscus appropriate for the growth of a plate having a desired half thickness
- pressure difference across the free surface to control the plate half thickness during the growth

APPENDIX

1. Proof of Statement 1.

Let $\alpha_c + \alpha_g < \pi/2$ and $z(x)$ defined for $x \in [x_c, x_d]$ which verifies (6) - (9) and $z''(x) > 0$ The function $\alpha(x) = -\arctan(z'(x))$ verifies $\alpha'(x) = (\rho \cdot g \cdot z + p)/(\gamma \cdot \cos\alpha)$ and the boundary conditions $\alpha(x_d) = \alpha_c$, $\alpha(x_c) = \pi/2 - \alpha_g$. Hence, by the mean value theorem, there is $x' \in [x_c, x_d]$ such that the following equality holds: $p = \gamma \cdot \frac{\alpha_c + \alpha_g - \pi/2}{x_d - xc} \cdot \cos\alpha(x') - \rho \cdot g \cdot z(x')$. On the other hand, inequality $z''(x) > 0$ implies that the function dz/dx is strictly increasing and by consequence the function $\alpha(x)$ is strictly decreasing. Therefore, $\alpha_c < \alpha(x') < \frac{\pi}{2} - \alpha_g$. Now, by taking into account that $z(x')$ >0 and $\gamma \cdot \frac{\alpha_c + \alpha_g - \pi/2}{x_d - x_c} < 0$ the following relations hold:

$$p = \gamma \cdot \frac{\alpha_c + \alpha_g - \pi/2}{x_d - x_c} \cdot \cos\alpha(x') - \rho \cdot g \cdot z(x') < \gamma \cdot \frac{\alpha_c + \alpha_g - \pi/2}{x_d - x_c} \cdot \cos\alpha(x') <$$

$$\gamma \cdot \frac{\alpha_c + \alpha_g - \pi/2}{x_d - x_c} \cdot \sin\alpha(\alpha_g) = \gamma \cdot \frac{\alpha_c + \alpha_g - \pi/2}{x_d} \cdot \frac{n}{n-1} \cdot \sin\alpha_g$$

with $n = x_d / x_c > 1$.

So, the right hand side of the inequality (11) is proven.

In order to obtain the left hand side of (11) remark first the inequality:

$$\gamma \cdot \frac{\alpha_c + \alpha_g - \pi/2}{x_d - x_c} \cdot \cos\alpha(x') - \rho \cdot g \cdot z(x') > \gamma \cdot \frac{\alpha_c + \alpha_g - \pi/2}{x_d - x_c} \cdot \cos\alpha_c - \rho \cdot g \cdot z(x_c).$$

The term $-\rho \cdot g \cdot z(x_c)$ can be evaluated applying the mean value theorem for the function $z(x)$ on $[x_c, x_d]$. It follows that there exists $x'' \in [x_c, x_d]$ such that $z(x_d) - z(x_c) = (x_d - x_c) \cdot z'(x'') > (x_d - x_c) \cdot z'(x_c) = -(x_d - x_c) \cdot \tan(\pi/2 - \alpha_g)$ with $z(x_d) = 0$.

Consequently, the following inequality holds:

$$-\rho \cdot g \cdot z(x_c) > -\rho \cdot g \cdot (x_d - x_c) \cdot \tan(\pi/2 - \alpha_g).$$

So, for p the following relations hold:

$$p=\gamma\cdot\frac{\alpha_c+\alpha_g-\pi/2}{x_d-x_c}\cdot\cos\alpha(x')-\rho\cdot g\cdot z(x')>\gamma\cdot\frac{\alpha_c+\alpha_g-\pi/2}{x_d-x_c}\cdot\cos\alpha_c-\rho\cdot g\cdot z(x_c)>$$
$$\gamma\cdot\frac{\alpha_c+\alpha_g-\pi/2}{x_d-x_c}\cdot\cos\alpha_c-\rho\cdot g\cdot(x_d-x_c)\cdot\tan\left(\pi/2-\alpha_g\right)=$$
$$\gamma\cdot\frac{\alpha_c+\alpha_g-\pi/2}{x_d}\cdot\frac{n}{n-1}\cdot\cos\alpha_c-\rho\cdot g\cdot x_d\cdot\frac{(n-1)}{n}\cdot\tan\left(\pi/2-\alpha_g\right)$$

This means that the left hand side of (11) is proven.

2. Proof of Statement 2. [14]

Since (6) is the Euler equation of the free energy functional given by (10) it is sufficient to prove that the Legendre and Jacobi conditions are satisfied in this case.

Denote by $F(z,z')=\gamma\cdot\left[1+(z')^2\right]^{1/2}-\rho\cdot g\cdot z^2/2-p\cdot z$.

It is easy to see that the Legendre condition in this case becomes $\gamma\cdot\left[1+(z')^2\right]^{-3/2}>0$ and so it is satisfied.

The Jacobi equation in this case becomes $\left(\gamma\cdot\left[1+(z')^2\right]^{-3/2}\cdot\eta'\right)'+\rho\cdot g\cdot\eta=0$. For the coefficients of this equation the following inequalities hold: $\gamma\cdot\left[1+(z')^2\right]^{-3/2}>\gamma\cdot\sin^3\alpha_g$ and $\rho\cdot g>0$. Therefore, the equation $\left(\gamma\cdot\sin^3\alpha_g\cdot\eta'\right)'+\rho\cdot g\cdot\eta=0$ is a Sturm type upper bound [14] for the Jacobi equation. An arbitrary solution of this last equation is given by $\eta(x)=A\cdot\sin(\omega\cdot x+\varphi)$ where A and φ are real constants and $\omega^2=\rho\cdot g/(\gamma\cdot\sin^3\alpha_g)$. The half period of this solution is equal to $\pi/\omega=\pi\cdot\gamma^{1/2}\sin^{3/2}\alpha_g/(\rho\cdot g)^{1/2}$. Inequality (15) implies that half period of $\eta(x)$ is more than x_d/n and so $\eta(x)$ vanishes at most once on the interval $[x_d/n,\,x_d]$. Since any non-zero solution of the equation $\left(\gamma\cdot\sin^3\alpha_g\cdot\eta'\right)'+\rho\cdot g\cdot\eta=0$ vanishes at most once on the interval $[x_d/n,\,x_d]$, the solution of the Jacobi equation $\left(\gamma\cdot\left[1+(z')^2\right]^{-3/2}\cdot\eta'\right)'+\rho\cdot g\cdot\eta=0$ which satisfies $\eta(x_d)=0,\ \eta'(x_d)=1$, has only one zero on the interval $[x_d/n,\,x_d]$. Hence the Jacobi condition is satisfied.

ACKNOWLEDGEMENT

This research did not receive any specific grant from funding agencies in the public, commercial, or not-for-profit sectors.

REFERENCES

[1] D. H. Yoon, I. Yonenga, T. Fukuda, H. Ohnishi, Crystal growth of dislocation-free $LiNbO_3$ single crystals by micro pulling down method, *Journal of Crystal Growth*, Volume **142**, Issues 3–4, Pages 339-343, 2 September 1994.

[2] Y. M. Yu, V. I. Chani, K. Shimamma, K. Inaba, T. Fukuda, Growth of vanadium garnet fiber crystals and variations of lattice parameter, *J. of Crystal Growth*, Vol **177**, Issues 1–2, Pages 74-78, 2 May 1997.

[3] B. M. Epelbaum, K. Imaba, S. Uda, T. Fukuda, A double-die modification of micro-pulling-down method for in situ clad/core doping of fiber crystal, *Journal of Crystal Growth*, Vol **179**, Issues 3–4, Pages 559-566, 2 August 1997.

[4] K. Shimamma, S. Uda, T. Yamada, S. Sakaguchi, T. Fukuda, Photoconductive Behavior in Smectic A Phase of 2-(4'-Heptyloxyphenyl)-6-Dodecylthiobenzothiazole, *Japanese Journal of Applied Physics*, Volume **35**, Part 2, Number 6A, 1996.

[5] N. Schafer, T. Yamada, K. Simamura, H. J. Koh, T. Fukuda, Growth of Si_xGe_{1-x} crystals by the micro-pulling-down method, Journal of Crystal Growth, Volume **166**, Issues 1–4, Pages 675-679, 1 September 1996.

[6] C. W. Lan, S. Uda, T. Fukuda, Theoretical analysis of the micro-pulling-down process for Ge_xSi_{1-x} fiber crystal growth, *Journal of Crystal Growth*, Volume **193**, Issue 4, Pages 552-562, 15 October 1998.

[7] B. M. Epelbaum, K. Shimamura, S. Uda, J. Kohn, T. Fukuda, Operating Limits for Stable Growth of Silicon Fibers with Diameter Less Than 150 μm by Modified μ-PD Method, *Crystal Research & Technology*, Volume **31**, Issue 8, Pages 1077-1084, 1996.

[8] H. J. Kohn, N. Shafer, K. Shimamura, T. Fukuda, $Si_{1-x}Ge_x$ fiber crystals with functionally variant composition grown by micro-pulling-down technique, *Journal of Crystal Growth*, Volume **167**, Issues 1–2, Pages 38-44, 2 September 1996.

[9] S. Uda, J. Kohn, K. Shimamura, T. Fukuda, Analysis of Ge distribution in $Si_{1-x}Ge_x$ single crystal fibers by the micro-pulling down method, *Journal of Crystal Growth*, Volume **167**, Issues 1–2, Pages 64-73, 2 September 1996.

[10] R. Finn, *Equilibrium capillary surfaces*, vol. **284** of *Grundlehren der mathematischen Wissenschaften*, Springer, New York, 1986.

[11]V. A. Tatarchenko, *Shaped crystal growth*, Kluwer Academic Publishers, Dordrecht, 1993.

[12] W.-K. Rhim, K. Ohsaka, Thermophysical properties measurement of molten silicon by high-temperature electrostatic levitator: density, volume expansion, specific heat capacity, emissivity, surface tension and viscosity, *Journal Crystal Growth*, Volume **208**, Issues 1–4, Pages 313-321, 1 January 2000.

[13] H. M. Ettouney, R. A. Brown, J. P. Kalejs, Analysis of operating limits in edge-defined film-fed crystal growth, *Journal of Crystal Growth*, Volume **62**, Issue 2, Pages 230-246, July 1983.

[14] P. Hartman, *Ordinary Differential Equations*, John Wiley & Sons, New York, NY, USA, 1964.